



Structural basis for multi-specific peptide recognition by the anti-IDH1/2 monoclonal antibody, MsMab-1



Yu Kitago ^a, Mika K. Kaneko ^b, Satoshi Ogasawara ^b, Yukinari Kato ^{b, **}, Junichi Takagi ^{a, *}

^a Laboratory of Protein Synthesis and Expression, Institute for Protein Research, Osaka University, 3-2 Yamadaoka, Suita, Osaka 565-0871, Japan

^b Department of Regional Innovation, Tohoku University Graduate School of Medicine, 2-1 Seiryomachi, Aoba-ku, Sendai, Miyagi 980-8575, Japan

ARTICLE INFO

Article history:

Received 10 August 2016

Accepted 18 August 2016

Available online 20 August 2016

Keywords:

Monoclonal antibody

X-ray crystallography

Multi-specificity

Isocitrate dehydrogenase

Tumor diagnosis

ABSTRACT

A point mutation in isocitrate dehydrogenase 1 (IDH1) and IDH2 is directly linked to the pathogenesis of certain types of tumors. To detect this mutation, several antibodies that can distinguish between mutant and wild-type enzymes have been established. One of which, MsMab-1, has a unique multi-specific character against several types of mutated IDH1/2. This promiscuous character is in remarkable contrast to the highly specific antigen recognition typically observed with a monoclonal antibody. We solved the crystal structure of MsMab-1 Fab fragment in complex with either IDH1 or IDH2-derived peptides. Based on the structure, it became clear that the peptide-binding pocket of the antibody is highly complementary to the core determinant shared between the IDH1 and IDH2, while leaving just enough space for the side chain of the pathogenic but not the wild-type amino acids located in the mutation position. Clarification of the molecular basis for the peculiar binding characteristics of MsMab-1 in atomic detail will help facilitating its diagnostic application, and may be used to develop better diagnostic reagents through structure-guided protein engineering.

© 2016 Elsevier Inc. All rights reserved.

1. Introduction

Isocitrate dehydrogenase 1 (IDH1) and IDH2 catalyze oxidative carboxylation of isocitrate into α -ketoglutarate in the cytosol and the mitochondria, respectively [1,2]. Interestingly, several point mutations within the IDH1/2 genes have been identified in cancerous cells isolated from patients with glioma, acute myeloid leukemia, and cartilaginous tumors [3–6]. Majority of these mutations occur in the same amino acid position (Arg¹³² in IDH1 and Arg¹⁷² in IDH2, Fig. 1A), converting them to several types of other amino acids. Especially in glioma, Arg¹³²/Arg¹⁷² is mutated to His, Cys, Ser, Gly, Met, and Lys [7]. It has been reported that the mutated IDH1/2 shows altered enzymatic property and produces D-2-hydroxyglutarate, which increases a risk of tumor malignancy [8,9].

Since there is a clear correlation between the mutation in the IDH1/2 and the pathogenesis, antibodies that can specifically recognize mutated but not wild-type enzymes are of great potential utility in the diagnostic or even the therapeutic applications. In fact,

several monoclonal antibodies against the mutated IDH1/2 have been established and their application to the cancer diagnosis is being discussed [10].

We have isolated multiple murine antibodies that bind to the Arg-to-Gly mutant of human IDH1 (IDH1-R132G) but not to the wild type enzyme, from mice immunized with a synthetic peptide containing the mutation. One of the established antibodies, MsMab-1 (mouse IgG_{2a}, κ), showed highly unique property in that it recognized several different IDH1 mutants without binding to the wild type version. Moreover, MsMab-1 could recognize several pathogenic IDH2 mutants without binding to the wild type IDH2 [11,12]. The broad specificity toward multiple pathogenic IDH1/2 mutants while maintaining a strict distinction from the wild-type enzyme suggests that this antibody may be used as a single diagnostic agent to detect various IDH mutations in a cancer specimen. We have already shown that the MsMab-1 can detect mutated IDH1/2 in glioma tissues by immunohistochemical staining, indicating its high potential in diagnostic applications [10,12]. Although the practical advantage of MsMab-1 in the cancer diagnosis is clear, it is difficult to reconcile that one antibody exhibits both highly selective and non-selective binding characters at the same time.

In this work, we performed structural analysis on the peptide binding by the MsMab-1 and clarified how the exclusive recognition of the mutated peptide was achieved while maintaining the

* Corresponding author.

** Corresponding author.

E-mail addresses: yukinari-k@bea.hi-ho.ne.jp (Y. Kato), takagi@protein.osaka-u.ac.jp (J. Takagi).

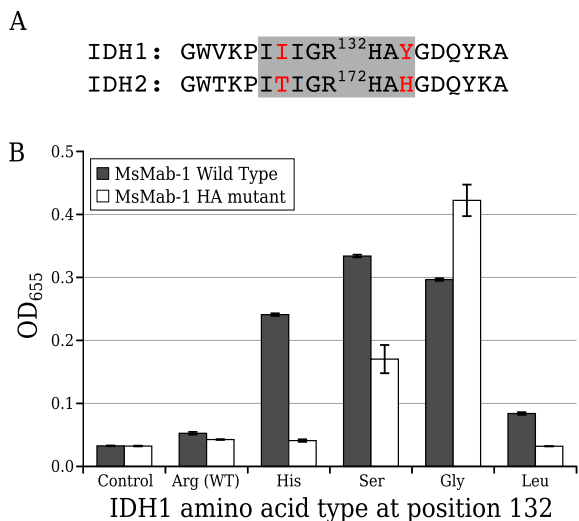


Fig. 1. Promiscuous recognition of IDH-derived peptide by MsMab-1. A, Amino acid sequences of human IDH1 and IDH2 near the pathogenic mutation position. The regions that are directly in contact with MsMab-1 is shaded in gray, with the two residues that differ between IDH1 and IDH2 shown in red. B, The binding ability of MsMab-1 against various peptides confirmed by ELISA. Binding of wild-type (filled bars) or HA mutant (open bars) versions of MsMab-1 IgG toward wells coated with 19-mer IDH1-derived peptides with indicated mutation was evaluated. Uncoated wells are used as control. Data are mean \pm SD ($n = 3$) from a representative experiment. (For interpretation of the references to colour in this figure legend, the reader is referred to the web version of this article.)

multi-specificity.

2. Materials and methods

2.1. IgG production and cloning

MsMab-1 was produced using mouse medial iliac lymph node methods, and its heavy and light chain genes were cloned as described previously [12]. Institutional animal committee of Tohoku University approved our study. The HA mutant of MsMab-1 was produced using a QuikChange Lightning site-directed mutagenesis kit (Agilent Technologies Inc., Santa Clara, CA). Chinese hamster ovary (CHO)-K1 cells (American Type Culture Collection (ATCC), Manassas, VA) were transfected with the plasmids using a Gene Pulser Xcell electroporation system (Bio-Rad Laboratories Inc., Berkeley, CA), and recombinant HA mutant of MsMab-1 was purified using Protein G-sepharose (GE Healthcare, Chicago, IL) from culture supernatant.

2.2. Enzyme-linked immunosorbent assay (ELISA)

Synthetic peptides (Sigma-Aldrich Corp., St. Louis, MO) were immobilized on Nunc Maxisorp 96-well immunoplates (Thermo Fisher Scientific Inc., Waltham, MA) at 1 μ g/ml for 30 min. Synthetic peptides are as follows: GGVKPIIIGRHAYGDQYRA (IDH1-WT), GGVKPIIIGHHAYGDQYRA (IDH1-R132H), GGVKPIIIGSHAYGDQYRA (IDH1-R132S), GGVKPIIIGGHAYGDQYRA (IDH1-R132G), GGVKPIIIGLHAYGDQYRA (IDH1-R132L). After blocking with SuperBlock T20 (PBS) Blocking Buffer in PBS (Thermo Fisher Scientific Inc.), the plates were incubated with purified mAbs (1 μ g/ml), followed by an incubation with peroxidase-conjugated anti-mouse IgG (1:1000 dilution, Agilent Technologies, Inc.). The enzymatic reaction was conducted with 1-Step Ultra TMB-ELISA (Thermo Fisher Scientific Inc.). The optical density was measured at 655 nm using an iMark microplate reader (Bio-Rad Laboratories Inc.).

2.3. Fab preparation and crystallization

To produce Fab fragment, MsMab-1 IgG was digested by papain (Papain-agarose: Thermo Fisher Scientific Inc.) in PE buffer (20 mM potassium sodium phosphate buffer pH 7.0, 10 mM EDTA) containing 25 mM Cys-HCl pH 7.0. After dialysis against TBS buffer (20 mM Tris-HCl pH 8.0, 150 mM NaCl), Fc fragment was removed from the digested mixture by Protein A-Sepharose (GE Healthcare), and the flow through fraction was desalted on a PD-10 column (GE Healthcare) and concentrated to \sim 10 mg/ml with an Amicon Ultra-15 ultrafiltration membrane (30 kDa MWCO; EMD Millipore Corp., Billerica, MA) before crystallization. For crystallization of the complex with a ligand peptide, 1/10 volume of 10 mM peptide dissolved in water was added to the purified Fab sample just before the crystallization. Synthetic peptides IDH1(Ser) (KPIIIGSHAYGD) and IDH2(Ser) (TKPITIGSHAHGDQYK) were purchased from Sigma-Aldrich Corp.

The crystallization screening of the IDH1(Ser)-Fab complex was performed using the sitting drop vapor diffusion method with the Index (Hampton Research, Aliso Viejo, CA) and Classics Neo (Qiagen, Hilden, Germany) kits. The initial condition was optimized, and diffraction-quality crystals were obtained under the condition of 0.1 M imidazole buffer pH 6.5 containing 2.0 M ammonium sulfate, 0.2 M potassium sodium tartrate with the hanging drop vapor diffusion method. The crystal for the IDH2(Ser)-Fab complex was obtained under the same condition. For the diffraction data collection, the crystals were soaked in the same solution containing 10%(v/v) ethylene glycol, and was rapidly frozen with liquid nitrogen.

2.4. X-ray data collection and processing

The diffraction data sets were collected at BL44XU beamline, SPring-8 (Hyogo, Japan), and the diffraction images were processed with XDS [13]. For the Fab-IDH1(Ser) complex, the initial phases were calculated by molecular replacement method with PHASER [14] using a Fab structure of mouse IgG_{2a} (PDID: 4EBQ) as a search model. The initial phases were then improved by density modification with DM [15], and an initial model was automatically built with ARP/wARP [16]. The model was refined with phenix.refine [17] and iterative manual editing using COOT [18]. For IDH2(Ser)-Fab complex, the initial phases were calculated by molecular replacement method using the structure of IDH1(Ser)-Fab as a search model, and the resultant model was refined with manual editing on COOT and REFMAC5 [19]. The model validation was carried out with MOLPROBITY [20], and all figures were prepared with PyMOL (<http://www.pymol.org/>). Diffraction data statistics and final refinement statistics are shown in Supplement Table 1.

3. Results and discussion

3.1. MsMab-1 Fab crystal structure with a mutant IDH1-derived peptide

We evaluated the binding of MsMab-1 toward various IDH1-derived 19-mer peptides by ELISA. As shown in Fig. 1B, MsMab-1 showed no binding toward wild-type peptide containing Arg132, but recognized peptides containing His, Ser, Leu and Gly at the same site (black bars). As the binding signal was the highest for the peptide with Ser substitution, we used a 12-mer peptide containing Ser mutation (designated as IDH1(Ser) hereafter) for the co-crystallization with the MsMab-1 Fab. Crystals grew under multiple conditions, and we successfully obtained diffraction quality crystals after optimization. From the diffraction dataset collected using the BL44XU at SPring-8, initial phases were calculated by

molecular replacement method, and the final structure was refined at the resolution of 1.93 Å. The crystal contained two copies of peptide-Fab complexes in the asymmetric unit. Electron densities were clearly visible for all 12 residues of IDH1(Ser) peptide bound to one Fab (molecule 1) in the asymmetric unit, while the C-terminal 2 residues of the peptide bound to the other Fab (molecule 2) were disordered. Nevertheless, the visible 10 residues had the same conformation in the two molecules. As the variable region of the antibody molecules were also virtually identical, we will only discuss the structure of the molecule 1 hereafter. We will also use the peptide residue numbering based on their original IDH sequence positions throughout the paper.

The MsMab-1 Fab fragment assumes a typical Fab structure consisting of four immunoglobulin-like β -sandwich domains, and the ligand peptide is packed into a pocket formed by CDR loops L2, L3, H1, and H3 (Fig. 2A). The peptide sits on a bent H3 (Fig. 2B), which is exceptionally short (4 residues) compared to typical H3 loops in the database [21,22]. This feature made the antigen binding groove narrow and deep, burying most of the surface of the antigen peptide. The N-terminal half of the peptide has extended conformation and lies along the narrow cleft between heavy and light chains. At Gly¹³¹ in the middle, the peptide backbone bends abruptly and forms single turn helix ascending from the bottom of the cleft (Fig. 2B), and

projects the C-terminal two residues that are disordered in the molecule 2 out of the pocket (Fig. 2C, asterisk). The side chains of peptide residues Ile¹²⁸, Ile¹³⁰, His¹³³, and Tyr¹³⁵ all made intimate VDW contacts with the surface of Fab (Fig. 2C, 2D), indicating their fundamental contribution to the interaction. The presence of Gly at the position 131 also seems essential, since its C α atom is in a direct contact with the floor of the cleft and presence of any side chain would not be tolerated (Fig. 2D). The side chain of the pathogenic mutation residue, Ser¹³², is pointing toward a cavity formed by the Fab and the Ile¹²⁹ of the peptide itself, with its hydroxyl oxygen making a direct hydrogen bond with His⁹⁵ (based on the Chothia's numbering scheme, [23]) of antibody heavy chain (Fig. 2C).

In order to simulate the binding of various IDH1 peptides, we modeled different side chains for the residue 132 based on the crystal structure of IDH1(Ser)-Fab complex (Fig. 3). When the mutations shown to be permissive for the MsMab-1 binding were introduced, the side chains were well accommodated in the cavity. However, the wild-type residue Arg is too large and expected to cause steric clash with either the antibody or the peptide itself. Therefore, the multi-specific property of MsMab-1 as well as its inability to recognize wild-type IDH1 is warranted by creating a right size of cavity through a unique cooperation between antigen binding pocket and the bound peptide itself.

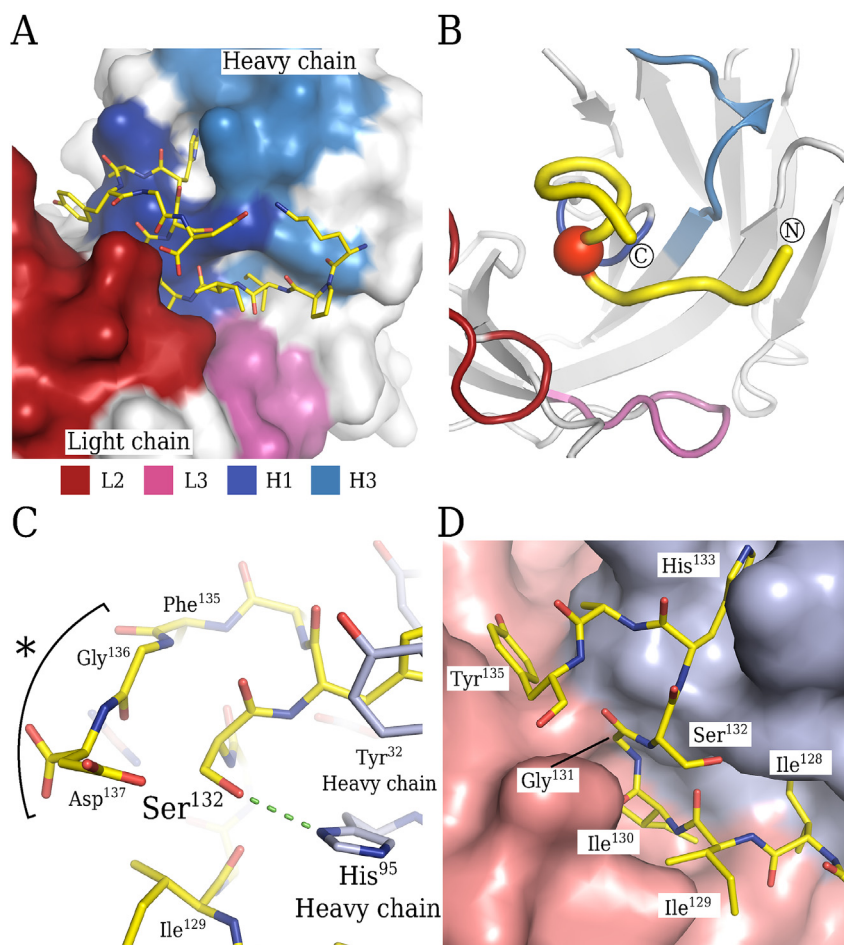


Fig. 2. Structure of MsMab-1 in complex with IDH1(Ser) peptide. A, IDH1(Ser) peptide (stick model with CPK coloring) recognized by MsMab-1 Fab (surface rendering) is shown. L2, L3, H1, and H3 loops are color-coded as indicated. H2 and L1 loops do not make contact with the peptide. B, An alternative view of A. Fab and IDH1(Ser) are shown as ribbon and a thick tube, respectively, with the same color-code as in A. The backbone of IDH1(Ser) bends abruptly at the Gly¹³¹ (red sphere). C, D, The close up views of the binding site near the Ser¹³². In C, a hydrogen bonding interaction between Ser¹³² and His⁹⁵H is shown as a green dashed line. The last two residues of IDH1(Ser) Gly¹³⁶ and Asp¹³⁷ (asterisk) are disordered in one of the complex in an asymmetric unit. In D, only the peptide segment corresponding to residues 127–135 is shown. The heavy chain and light chain surface of Fab are colored by light blue and pink, respectively. (For interpretation of the references to colour in this figure legend, the reader is referred to the web version of this article.)

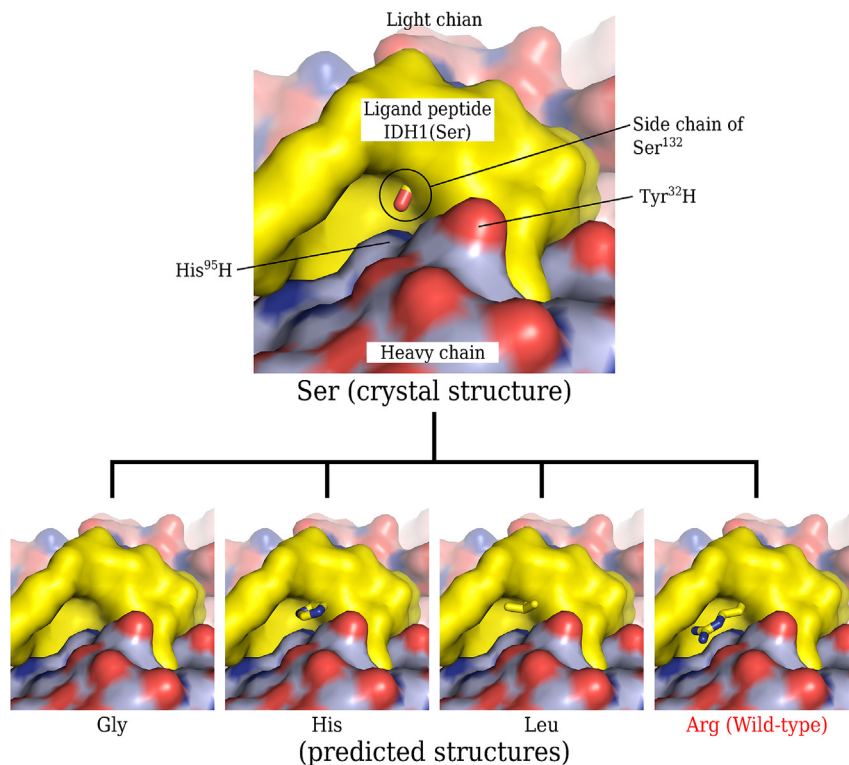


Fig. 3. Docking simulation of various IDH1 mutant peptides. In order to simulate the binding of various mutant IDH1 peptides, crystal structure of MsMab-1 Fab is shown in a surface model with CPK color scheme with the bound peptide portion modified to remove the Ser¹³² side chain (i.e., equivalent to Ser to Gly mutation) rendered in yellow surface. The top panel represents the actual crystal structure obtained with IDH1(Ser) where Ser side chain is shown in stick model. The bottom four panels each represent hypothetical docking model of peptide containing various amino acid residues including Gly, His, Leu, and Arg (= wild type) at position 132. (For interpretation of the references to colour in this figure legend, the reader is referred to the web version of this article.)

3.2. Ala substitution for His⁹⁵ of heavy chain changes ligand recognition property

On the Fab side, the H3 loop residue His⁹⁵ constitute the wall of the cavity described above, and defines its volume (Fig. 3). We speculated that changing the side chain of His⁹⁵ to a smaller one may enlarge the cavity, enabling a design of mutant antibody with a broader specificity. To test this hypothesis, we prepared a recombinant mutant MsMab-1 containing Ala in place of His⁹⁵ (HA mutant). The HA mutant version of MsMab-1 IgG was stably expressed using CHO-K1 cells, and purified from the culture supernatant (with a typical yield of 0.5 mg from 2 L media). In a separate experiment, we also confirmed that the original wild-type MsMab-1 can be recombinantly produced at similar level (data now shown), indicating that the mutation does not affect the stability of the antibody. The purified HA MsMab-1 was evaluated for the binding toward different IDH1 peptides by using the same ELISA format as the original MsMab-1 (Fig. 1B, white bars). Contrary to our expectation, the mutant antibody did not show broader specificity than the original antibody; rather, the specificity became narrower because the HA MsMab-1 could only bind peptides carrying Gly and Ser at the position 132. We note that Tyr³² in the H1 loop sits right next to the His⁹⁵, with its side chain phenolic ring pushed back by the His⁹⁵ imidazole (Fig. 3). Retrospectively, the vacancy created by the removal of the His⁹⁵ side chain would be readily filled by that of Tyr³², making the cavity even smaller. Although our simple subtraction strategy of structure-guided re-engineering to obtain an antibody with a desired property did not work, the result confirmed the essential role of His⁹⁵ in discriminating amino acid types present in the residue 132 of IDH1, validating our crystal structure.

3.3. Crystal structure of MsMab-1 Fab in complex with mutated IDH2-derived peptide

The remaining puzzle about the promiscuous binding properties of MsMab-1 is its ability to recognize pathogenic IDH2 peptide whose sequence is similar but distinct from that of IDH1. Within the 10-residue region of IDH1 peptide making direct contact with the MsMab-1, sequence variations exist at two positions; the Ile¹²⁹ and Tyr¹³⁵ in IDH1 are replaced by Thr¹⁶⁹ and His¹⁷⁵ in IDH2, respectively (Fig. 1A). The first position (Ile¹²⁹) exposes its side chain group to the solvent, suggesting that the Thr residue of IDH2 is allowed in this position (Fig. 2D). However, the side chain of the second position (Tyr¹³⁵) contributes significantly to the interaction, by a hydrophobic packing with the side chain of Ile⁵⁵ from the L2 loop as well as a water-mediated hydrogen bonding network involving main chain carbonyls (Fig. 4A). To understand the mechanism underlying the dual-specificity, we crystallized MsMab-1 Fab in the presence of a 16-mer IDH2-derived peptide containing a pathogenic Arg-to-Ser mutation at the residue 172 (i.e., IDH2(Ser)). From the crystal structure solved at a resolution of 1.93 Å, it became clear that the antibody indeed recognized IDH2-derived peptide in a manner indistinguishable from that of IDH1 peptide (Fig. 4B). First, the Fv part of the antibody superimposes with that of the IDH1(Ser)-complex with an RMSD value of 0.39 Å for a total of 215 residues, and virtually no difference is observed for the conformation of the side chains of all residues making direct contacts with the ligand peptides (Fig. 4C). This indicates that the antibody does not adjust its structure for the recognition of two different peptides. At the peptide side, the central 10 residues (Pro¹⁶⁷-Gly¹⁷⁶) are visible in the electron density map. When superposed onto the Fab-IDH1(Ser) complex structure using the Fv

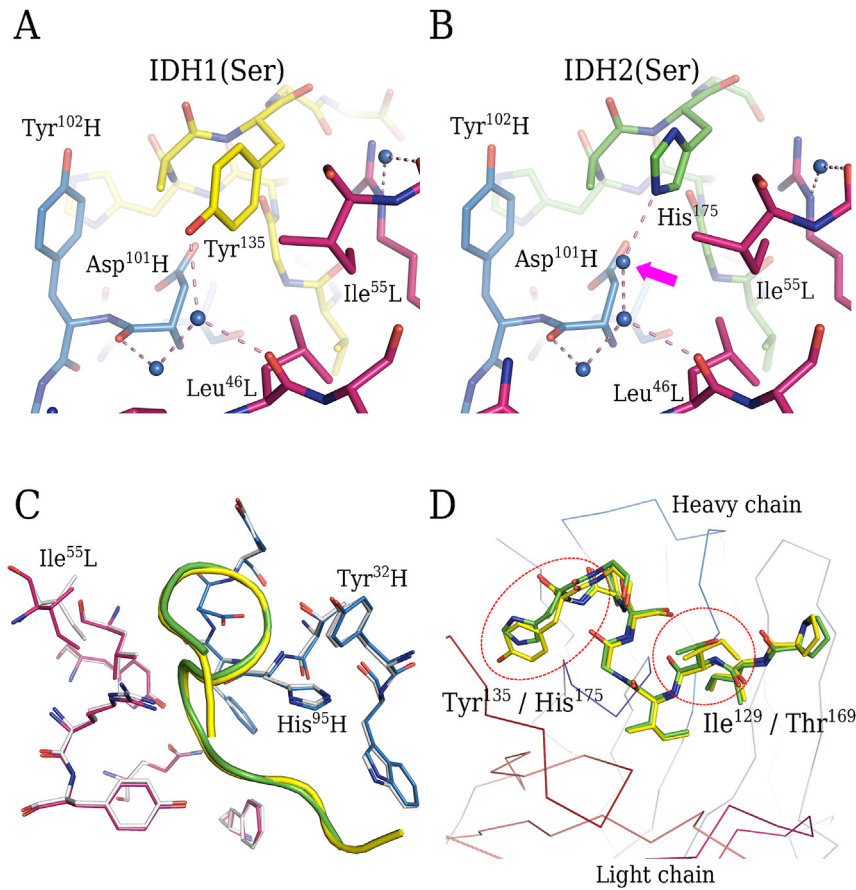


Fig. 4. Structural comparison between MsMab-1 bound by IDH1(Ser) and IDH2(Ser). A, B, The close-up views of the recognition environment for the isotype-specific residue Tyr¹³⁵ in IDH1 (A) and His¹⁷⁵ in IDH2 (B). Water molecules (blue spheres) and hydrogen bonds (pink dashed lines) are shown. A and B are viewed from the same orientation after structurally aligning the Fv portions. C, Superposition of the two complex structures. The antibody residues making direct contacts with IDH1(Ser) peptide (yellow tube) are shown in blue (H chain) and red (light chain) stick models, respectively, and the corresponding residues in the IDH2(Ser) (green tube) complex are in white color. D, Conformation of the IDH1(Ser) (yellow) and IDH2(Ser) (green) peptides bound onto MsMab-1 (C α trace). Only the peptide segments that are present in both structures are shown. Residues that differ between the isoforms (Tyr¹³⁵/His¹⁷⁵ and Ile¹²⁹/Thr¹⁶⁹) are indicated by red dashed circles. (For interpretation of the references to colour in this figure legend, the reader is referred to the web version of this article.)

portion, the two peptides have essentially identical conformation, showing an RMSD value of 0.20 Å for 10 matched C α atoms. As expected, Thr¹⁶⁹ is pointing away from the antibody, consistent with the lack of peptide discrimination at this position (Fig. 4D). For the second subtype-specific residue, the His¹⁷⁵ perfectly emulates conformation of the Tyr¹³⁵ and keep the same ring stacking with the Ile^{55L} (Fig. 4A,B,D). Furthermore, acquisition of an additional water restored the hydrogen bonding network, making the interface virtually identical despite the Tyr to His replacement (Fig. 4B). Thus, we conclude that MsMab-1 accomplishes the dual specificity by recognizing common structural feature shared between IDH1 and IDH2. Furthermore, the structural environment of the pathogenic mutation residue is conserved between IDH1 and IDH2, explaining why MsMab-1 exhibits promiscuity (i.e., the dual recognition and the large choice of amino acid at the mutation position) without recognizing the wild-type IDH1/2 proteins.

The point mutation at Arg¹³² of IDH1 and Arg¹⁷² of IDH2 is commonly observed in 50–80% of gliomas [7]. A rapid detection of this mutation in a patient is necessary to enable accurate diagnosis required for designing appropriate therapeutic strategies. Particularly, the diagnosis by the immunohistochemical staining of a pathological tissue sample is considered superior to the genetic analysis of the patient, because it can be implemented more easily in a wide variety of clinical situations. Although the potential of using the immunohistochemistry in the diagnosis of gliomas has been

postulated [24], there is one drawback to this method. So far, specific antibodies for several pathogenic mutated IDHs have been developed and commercially available. However, since over ten types of pathogenic mutation at the key Arg residue have been reported on both IDH1 and IDH2, one must search for many different antigens in a tissue specimen. So far, antibodies specific for several pathogenic mutated, but not wild-type, sequences of IDH have been developed and commercially available. Each antibody was raised against individual mutant sequence, and must be used in combination or as a mixture to detect unknown mutation. In contrast, the MsMab-1 can be used alone to detect many disease-causing mutations in both IDH1 and IDH2, simplifying the diagnostic procedure. Although this property was counter-intuitive due to the well-established antibody's role as a highly selective binder, our structural analyses unraveled the mechanism underlying this seemingly puzzling phenomenon. It is anticipated that the structural information obtained in this study can be used to engineer better antibodies with improved affinity and/or modified specificity, contributing to the development of easy and accurate diagnostic tools for human glioma.

Accession codes

Coordinates and structure factors have been deposited in the Protein Data Bank under accession codes 5GIR for MsMab-1 Fab with IDH1(Ser), and 5GIS for MsMab-1 Fab with IDH2(Ser).

Funding

This work was supported in part by the “Platform for Drug Discovery, Informatics, and Structural Life Science” grant from the Japan Agency for Medical Research and Development (AMED) to J.T. and Y.Ka., by Practical Research for Innovation Cancer Control from Japan Agency for Medical Research and development, AMED (Y. Ka.), by JSPS KAKENHI Grant Number 25462242 and 16K10748 (Y.Ka.), by the Regional Innovation Strategy Support Program from the Ministry of Education, Culture, Sports, Science and Technology (MEXT) of Japan (Y.Ka.), and by the Basic Science and Platform Technology Program for Innovative Biological Medicine from AMED (Y.Ka.). This work was performed under the Cooperative Research Program of Institute for Protein Research, Osaka University (CR15-05).

Acknowledgement

We would like to thank Dr. Yamashita, Dr. Higashiura, and Dr. Nakagawa at SPring-8 BL44XU for their help with X-ray data collection.

Transparency document

Transparency document related to this article can be found online at <http://dx.doi.org/10.1016/j.bbrc.2016.08.110>.

Appendix A. Supplementary data

Supplementary data related to this article can be found at <http://dx.doi.org/10.1016/j.bbrc.2016.08.110>

References

- [1] N.S. Henderson, Isozymes of isocitrate dehydrogenase - subunit structure and intracellular location, *J. Exp. Zool.* 158 (1965) 263–273.
- [2] B.V. Geisbrecht, S.J. Gould, The human PICD gene encodes a cytoplasmic and peroxisomal NADP(+)-dependent isocitrate dehydrogenase, *J. Biol. Chem.* 274 (1999) 30527–30533.
- [3] H. Yan, D.W. Parsons, G.L. Jin, R. McLendon, B.A. Rasheed, W.S. Yuan, I. Kos, I. Batinic-Haberle, S. Jones, G.J. Riggins, H. Friedman, A. Friedman, D. Reardon, J. Herndon, K.W. Kinzler, V.E. Velculescu, B. Vogelstein, D.D. Bigner, IDH1 and IDH2 mutations in gliomas, *N Engl. J. Med.* 360 (2009) 765–773.
- [4] D.W. Parsons, S. Jones, X.S. Zhang, J.C.H. Lin, R.J. Leary, P. Angenendt, P. Mankoo, H. Carter, I.M. Siu, G.L. Gallia, A. Olivi, R. McLendon, B.A. Rasheed, S. Keir, T. Nikolskaya, Y. Nikolsky, D.A. Busam, H. Tekleab, L.A. Diaz, J. Hartigan, D.R. Smith, R.L. Strausberg, S.K.N. Marie, S.M.O. Shinjo, H. Yan, G.J. Riggins, D.D. Bigner, R. Karchin, N. Papadopoulos, G. Parmigiani, B. Vogelstein, V.E. Velculescu, K.W. Kinzler, An integrated genomic analysis of human glioblastoma multiforme, *Science* 321 (2008) 1807–1812.
- [5] E.R. Mardis, L. Ding, D.J. Dooling, D.E. Larson, M.D. McLellan, K. Chen, D.C. Koboldt, R.S. Fulton, K.D. Delehaunty, S.D. McGrath, L.A. Fulton, D.P. Locke, V.J. Magrini, R.M. Abbott, T.L. Vickery, J.S. Reed, J.S. Robinson, T. Wyllie, S.M. Smith, L. Carmichael, J.M. Eldred, C.C. Harris, J. Walker, J.B. Peck, F.Y. Du, A.F. Dukes, G.E. Sanderson, A.M. Brummett, E. Clark, J.F. McMichael, R.J. Meyer, J.K. Schindler, C.S. Pohl, J.W. Wallis, X.Q. Shi, L. Lin, H. Schmidt, Y.Z. Tang, C. Haipek, M.E. Wiechert, J.V. Ivy, J. Kalicki, G. Elliott, R.E. Ries, J.E. Payton, P. Westervelt, M.H. Tomasson, M.A. Watson, J. Baty, S. Heath, W.D. Shannon, R. Nagarajan, D.C. Link, M.J. Walter, T.A. Graubert, J.F. DiPersio, R.K. Wilson, T.J. Ley, Recurring mutations found by sequencing an acute myeloid leukemia genome, *N. Engl. J. Med.* 361 (2009) 1058–1066.
- [6] M.F. Amary, K. Bacsi, F. Maggiani, S. Damato, D. Halai, F. Berisha, R. Pollock, P. O'Donnell, A. Grigoriadis, T. Diss, M. Eskandarpour, N. Presneau, P.C. Hogendoorn, A. Futreal, R. Tirabosco, A.M. Flanagan, IDH1 and IDH2 mutations are frequent events in central chondrosarcoma and central and periosteal chondromas but not in other mesenchymal tumours, *J. Pathol.* 224 (2011) 334–343.
- [7] H. Arita, Y. Narita, A. Yoshida, N. Hashimoto, T. Yoshimine, K. Ichimura, IDH1/2 mutation detection in gliomas, *Brain Tumor Pathol.* 32 (2015) 79–89.
- [8] L. Dang, D.W. White, S. Gross, B.D. Bennett, M.A. Bittinger, E.M. Driggers, V.R. Fantin, H.G. Jang, S. Jin, M.C. Keenan, K.M. Marks, R.M. Prins, P.S. Ward, K.E. Yen, L.M. Liu, J.D. Rabinowitz, L.C. Cantley, C.B. Thompson, M.G. Vander Heiden, S.M. Su, Cancer-associated IDH1 mutations produce 2-hydroxyglutarate, *Nature* 462 (2009) 739–744.
- [9] B. Yang, C. Zhong, Y.J. Peng, Z. Lai, J.P. Ding, Molecular mechanisms of “off-on switch” of activities of human IDH1 by tumor-associated mutation R132H, *Cell Res.* 20 (2010) 1188–1200.
- [10] Y. Kato, Specific monoclonal antibodies against IDH1/2 mutations as diagnostic tools for gliomas, *Brain Tumor Pathol.* 32 (2015) 3–11.
- [11] X. Liu, Y. Kato, M. Kato-Kaneko, M. Sugawara, S. Ogasawara, Y. Tsujimoto, Y. Naganuma, M. Yamakawa, T. Tsuchiya, M. Takagi, Isocitrate dehydrogenase 2 mutation is a frequent event in osteosarcoma detected by a multi-specific monoclonal antibody MsMab-1, *Cancer Med.* 2 (2013) 803–814.
- [12] M. Kato Kaneko, S. Ogasawara, Y. Kato, Establishment of a multi-specific monoclonal antibody MsMab-1 recognizing both IDH1 and IDH2 mutations, *Tohoku, J. Exp. Med.* 230 (2013) 103–109.
- [13] W. Kabsch, Xds, *Acta. Crystallogr. D. Biol. Crystallogr.* 66 (2010) 125–132.
- [14] A.J. McCoy, R.W. Grosse-Kunstleve, P.D. Adams, M.D. Winn, L.C. Storoni, R.J. Read, Phaser crystallographic software, *J. Appl. Cryst.* 40 (2007) 658–674.
- [15] K.D. Cowtan, ‘dm’: an automated procedure for phase improvement by density modification, *Jt. CCP4 + ESF-EACBM Newsletter on Protein Crystallography* 31 (1994) 34–38.
- [16] A. Perrakis, R. Morris, V.S. Lamzin, Automated protein model building combined with iterative structure refinement, *Nat. Struct. Biol.* 6 (1999) 458–463.
- [17] P.D. Adams, P.V. Afonine, G. Bunkoczi, V.B. Chen, I.W. Davis, N. Echols, J.J. Headd, L.W. Hung, G.J. Kapral, R.W. Grosse-Kunstleve, A.J. McCoy, N.W. Moriarty, R. Oeffner, R.J. Read, D.C. Richardson, J.S. Richardson, T.C. Terwilliger, P.H. Zwart, PHENIX: a comprehensive Python-based system for macromolecular structure solution, *Acta. Crystallogr. D. Biol. Crystallogr.* 66 (2010) 213–221.
- [18] P. Emsley, B. Lohkamp, W.G. Scott, K. Cowtan, Features and development of coot, *Acta. Crystallogr. D. Biol. Crystallogr.* 66 (2010) 486–501.
- [19] G.N. Murshudov, P. Skubak, A.A. Lebedev, N.S. Pannu, R.A. Steiner, R.A. Nicholls, M.D. Winn, F. Long, A.A. Vagin, REFMAC5 for the refinement of macromolecular crystal structures, *Acta. Crystallogr. D. Biol. Crystallogr.* 67 (2011) 355–367.
- [20] V.B. Chen, W.B. Arendall, J.J. Headd, D.A. Keedy, R.M. Immormino, G.J. Kapral, L.W. Murray, J.S. Richardson, D.C. Richardson, MolProbity: all-atom structure validation for macromolecular crystallography, *Acta. Crystallogr. D. Biol. Crystallogr.* 66 (2010) 12–21.
- [21] A.V.J. Collis, A.P. Brouwer, A.C.R. Martin, Analysis of the antigen combining site: correlations between length and sequence composition of the hypervariable loops and the nature of the antigen, *J. Mol. Biol.* 325 (2003) 337–354.
- [22] M. Zemlin, M. Klinger, J. Link, C. Zemlin, K. Bauers, J.A. Engler, H.W. Schroeder, P.M. Kirkham, Expressed murine and human CDR-H3 intervals of equal length exhibit distinct repertoires that differ in their amino acid composition and predicted range of structures, *J. Mol. Biol.* 334 (2003) 733–749.
- [23] C. Chothia, A.M. Lesk, Canonical structures for the hypervariable regions of immunoglobulins, *J. Mol. Biol.* 196 (1987) 901–917.
- [24] S. Takano, E. Ishikawa, N. Sakamoto, M. Matsuda, H. Akutsu, M. Noguchi, Y. Kato, T. Yamamoto, A. Matsumura, Immunohistochemistry on IDH 1/2, ATRX, p53 and Ki-67 substitute molecular genetic testing and predict patient prognosis in grade III adult diffuse gliomas, *Brain Tumor Pathol* 33 (2016) 107–116.